

# Mutations in the novel protocadherin *PCDH15* cause Usher syndrome type 1F

Kumar N. Alagramam, Huijun Yuan<sup>1</sup>, Markus H. Kuehn<sup>2</sup>, Crystal L. Murcia<sup>3</sup>, Sigrid Wayne<sup>1</sup>, C.R. Srikumari Srisailpathy<sup>1,5</sup>, R. Brian Lowry<sup>6</sup>, Russell Knaus<sup>7</sup>, Lut Van Laer<sup>8</sup>, F.P. Bernier<sup>6</sup>, Stuart Schwartz<sup>3,4</sup>, Charles Lee<sup>9</sup>, Cynthia C. Morton<sup>9</sup>, Robert F. Mullins<sup>2</sup>, Arabandi Ramesh<sup>1,5</sup>, Guy Van Camp<sup>8</sup>, Gregory S. Hagemen<sup>2</sup>, Richard P. Woychik<sup>10</sup> and Richard J.H. Smith<sup>1,\*</sup>

Department of Pediatrics, Rainbow Babies and Children's Hospital, University Hospitals of Cleveland, Case Western Reserve University, Cleveland, OH, USA, <sup>1</sup>Molecular Otolaryngology Research Laboratories, Department of Otolaryngology, University of Iowa, 200 Hawkins Drive, Iowa City, IA 52242, USA, <sup>2</sup>The University of Iowa Center for Macular Degeneration in the Department of Ophthalmology and Visual Sciences, University of Iowa, Iowa City, IA, USA, <sup>3</sup>Department of Genetics and <sup>4</sup>Center for Human Genetics, Case Western Reserve University and University Hospitals of Cleveland, Cleveland, OH, USA, <sup>5</sup>Department of Genetics, University of Madras, Madras, India, <sup>6</sup>Department of Genetics, Alberta Children's Hospital, Calgary, Alberta, Canada, <sup>7</sup>Lumsden Clinic, Lumsden, Saskatchewan, Canada, <sup>8</sup>Department of Genetics, University of Antwerp, Belgium, <sup>9</sup>Department of Obstetrics and Gynecology, Brigham and Women's Hospital, Harvard Medical School, Boston, MA, USA and <sup>10</sup>Lynx Therapeutics Inc., 25861 Industrial Boulevard, Hayward, CA 94545, USA.

Received May 14, 2001; Revised and Accepted June 11, 2001

**We have determined the molecular basis for Usher syndrome type 1F (USH1F) in two families segregating for this type of syndromic deafness. By fluorescence *in situ* hybridization, we placed the human homolog of the mouse protocadherin *Pcdh15* in the linkage interval defined by the *USH1F* locus. We determined the genomic structure of this novel protocadherin, and found a single-base deletion in exon 10 in one USH1F family and a nonsense mutation in exon 2 in the second. Consistent with the phenotypes observed in these families, we demonstrated expression of *PCDH15* in the retina and cochlea by RT-PCR and immunohistochemistry. This report shows that protocadherins are essential for maintenance of normal retinal and cochlear function.**

## INTRODUCTION

Usher syndrome is the most common cause of the dual sensory impairments of deafness and blindness. Affected persons are born with hearing loss and develop progressive pigmentary retinopathy leading to blindness in the second to fourth decades of life. Clinically subdivided into types 1–3 based on the degree of deafness and the presence of vestibular dysfunction, Usher syndrome type 1 (USH1) is the most severe (1). Persons with USH1 are born with profound deafness and develop visual problems in late childhood. Approximately

70% segregate for mutations in myosin 7A (USH1B); the second largest contribution to the USH1 genetic load is closely linked to the USH1D–USH1F region on chromosome 10 (2).

Several years ago we mapped the Usher syndrome type 1F (*USH1F*) locus in a complex family belonging to the Hutterite Brethren (3), an endogamous ethnic group which maintains a communal way of life on the prairies of central Canada and the USA (4,5). In the pedigree we studied, two males were born with profound sensorineural deafness and delayed developmental motor milestones suggesting the diagnosis of Usher syndrome. When the boys were older this clinical impression was confirmed by ophthalmologic evaluation, which revealed fundoscopic findings of retinitis pigmentosa and electroretinographic abnormalities. On a genome-wide screen, we found only one interval of homozygosity by descent, a 15 cM region on chromosome 10 flanked by markers D10S199 and D10S596. The LOD score over this interval was 3.06, and the locus was assigned the designation *USH1F*. We also linked a consanguineous USH1 family from India to this genomic region with a LOD score >3.0 (Fig. 1).

Recently, we reported cloning a novel murine protocadherin, *Pcdh15*, mutations in which are found in the Ames waltzer (*av*) mouse mutant and lead to a phenotype characterized by deafness and vestibular dysfunction associated with degeneration of inner ear neuro-epithelia (6,7). Using a mouse *Pcdh15* cDNA probe to screen a human genomic P1-derived artificial chromosome (PAC) library, we identified several clones of the human homolog, *PCDH15*, which we mapped to chromosome 10q11.2–q21 by fluorescence *in situ* hybridization (FISH).

\*To whom correspondence should be addressed. Tel: +1 319 356 3612; Fax: +1 319 356 4547; Email: richard-smith@uiowa.edu  
The authors wish it to be known that, in their opinion, the first two authors should be regarded as joint First Authors.



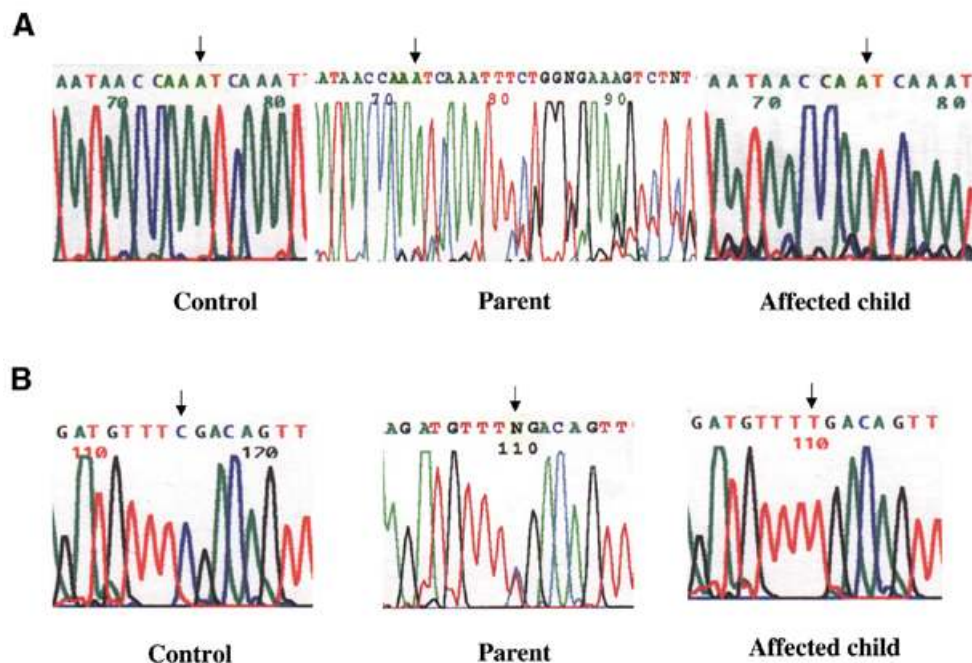


**Figure 2.** Sequencing results for *PCDH15*. (A) In the Hutterite family, a portion of the electropherogram for *PCDH15* exon 10 demonstrates the deletion of a thymidine at nucleotide 1471 (arrow, reverse strand shown), changing the reading frame and creating a stop codon after amino acid 419 in exon 11. (B) In the Indian family, a portion of the electropherogram for *PCDH15* exon 2 shows a C→T transition (arrow, forward strand shown), generating in a premature stop codon (TGA) after the second amino acid.

library, we presume that *PCDH15* is expressed in human fetal brain as well. Additional experiments by RT-PCR and direct sequencing also revealed expression in other human adult tissues (Fig. 3B) and human fetal cochlea.

Western blot analysis using an affinity-purified peptide antibody confirmed expression of the protein in brain, lung and kidney (Fig. 3C). The antibody, Pcadh15-PAb4, was raised in rabbits against peptide sequence TEDAHESEKEGGH-RDTLIV from the C-terminus of Pcdh15. The results showed that specific bands are recognized by Pcadh15-PAb4 (Fig. 3C). When incubated with the primary antibody, a band close to the expected size (~175 kDa) was seen; a duplicate blot incubated with the primary antibody pre-absorbed with the peptide antigen did not show this band. The other high molecular weight bands (180, 160 and 130 kDa) seen on the blot may be isoforms of *PCDH15*, since alternatively spliced products derived from *PCDH15* were detected by northern (Fig. 3A) and RT-PCR analyses (data not shown). The low molecular weight bands (<130 kDa) appeared as robust protein bands on the Coomassie blue-stained gel, and because they were seen on both panels, we believe they represent non-specific adsorption of secondary antibody to concentrated protein.

By immunohistochemistry, we detected *PCDH15* expression in the inner and outer synaptic layers and the nerve fiber layer in human adult and fetal retinas. Additional reactivity in the region of the outer limiting membrane/photoreceptor cell inner segments was observed in the adult but not the fetal retina (Fig. 3D). In human fetal cochlea, we detected *PCDH15* expression in the supporting cells and outer sulcus cells, as well as in the spiral ganglion. We confirmed these findings on

mouse cochlea, which also revealed expression on the apical surface of the hair cells (Fig. 3E).

#### Predicted amino acid sequence of *PCDH15*

*PCDH15* cDNA encodes an open reading frame (ORF) that translates to 1955 amino acids. The predicted protein has 11 cadherin repeats, one transmembrane domain and a cytoplasmic domain that contains two proline-rich regions (Fig. 4A). This organization is highly similar to the predicted protein for mouse *Pcdh15*.

We used phylogenetic analysis to determine the evolutionary relationship between *PCDH15* and the cadherin superfamily by comparing *PCDH15* to other protocadherins and cadherin-like sequences. Sequences were selected based on BLAST analysis or because the gene product was associated with a disease phenotype similar to *USH1F*, such as *CDH23* (*USH1D*) (8) (Fig. 4B).

These data show that *PCDH15* is related only distantly to other proteins, making it a unique member of the cadherin superfamily. This finding is consistent with the genomic organization of *PCDH15*, which differs from that of the human protocadherin gene clusters  $\alpha$ ,  $\beta$  and  $\gamma$ . In *PCDH15* the extracellular domain is encoded by several exons, whereas in the gene clusters, the extracellular and transmembrane domains are encoded by a single unusually large exon (9).

#### DISCUSSION

*PCDH15* is a novel member of the cadherin superfamily of calcium-dependent cell-cell adhesion molecules. Based on the phenotype observed in the *USH1F* families we studied, we

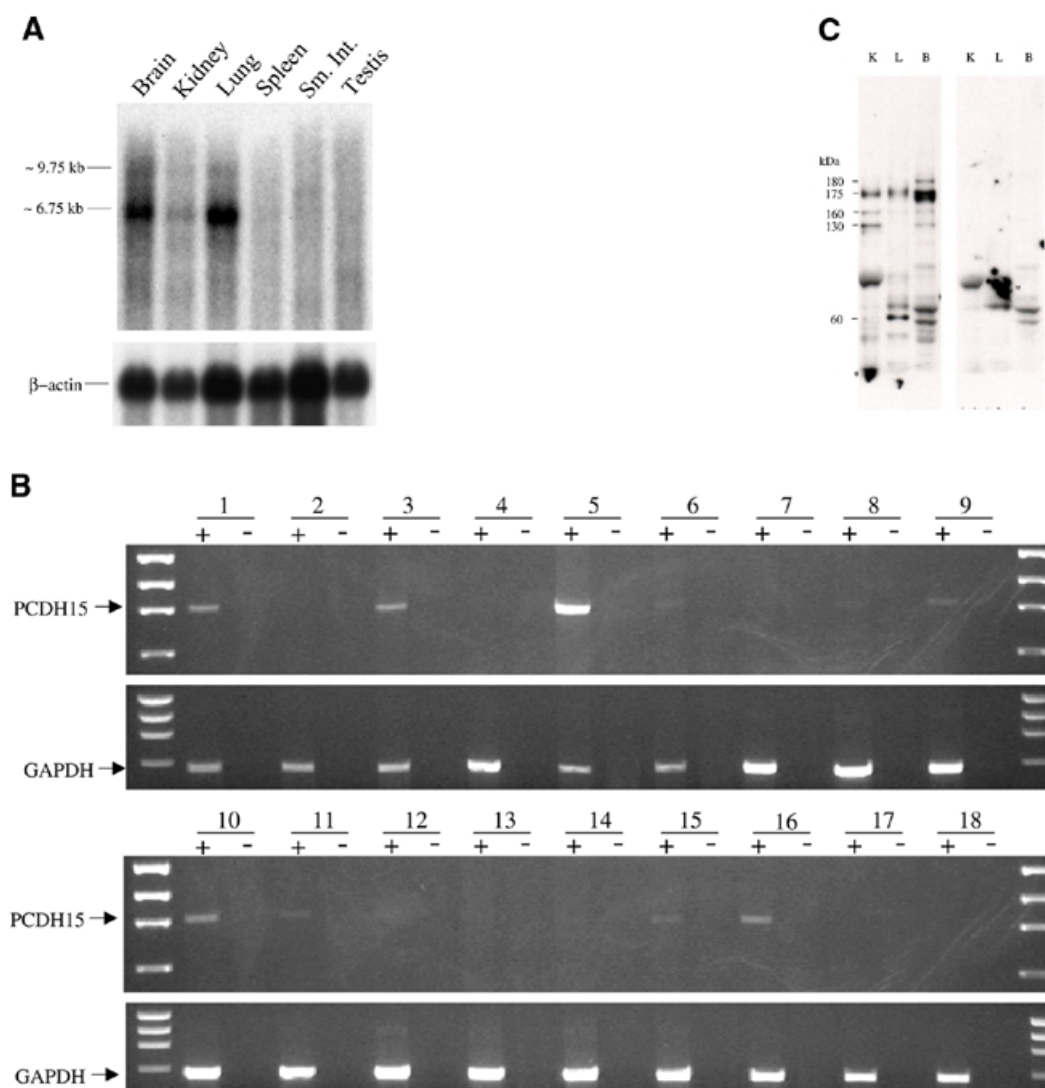
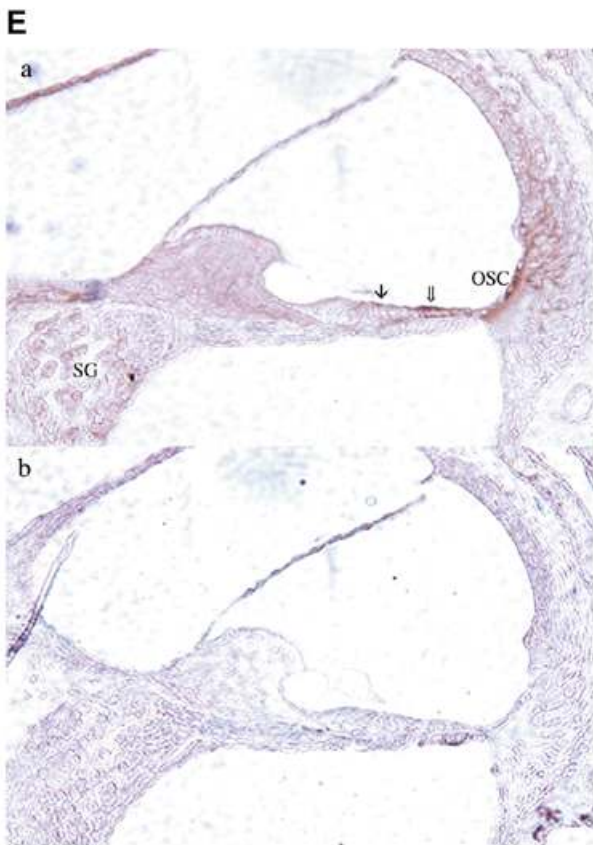
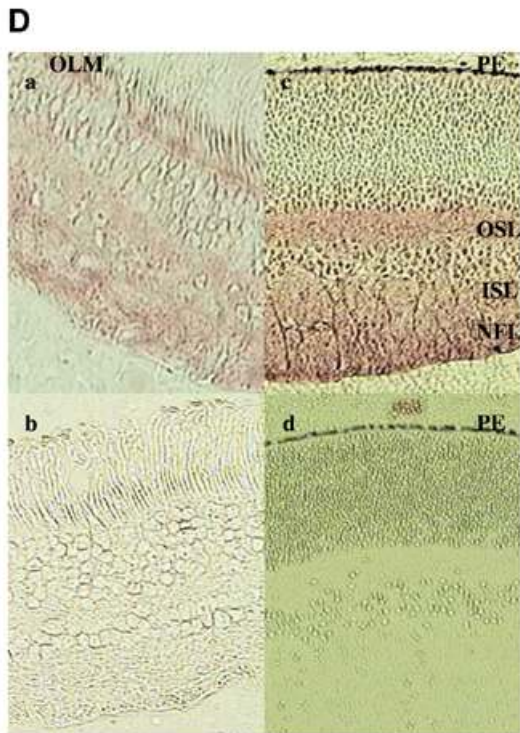


**Figure 3.** (A) Northern blot analysis demonstrating expression of *PCDH15* in different human tissues using 5  $\mu$ g A+ RNA per lane. Blots were hybridized with a 4 kb *PCDH15* cDNA probe; the same blot was then stripped and re-probed with human  $\beta$ -actin as the loading control. (B) RT-PCR demonstrating expression of *PCDH15* in total RNA isolated from adult human tissues (RNA was obtained from Clontech Human RNA panels I, II and III). 1, brain; 2, heart; 3, kidney; 4, liver; 5, lung; 6, trachea; 7, bone marrow; 8, colon; 9, small intestine; 10, spleen; 11, stomach; 12, thymus; 13, mammary gland; 14, prostate; 15, skeletal muscle; 16, testis; 17, uterus; 18, heart; size marker, PhiX174 digested with *Hae*III (Promega); band indicated by solid arrow, 1.078 kb. (C) Western blot analysis of adult human kidney (K), lung (L) and brain (B) probed with mouse peptide antibody, Pcdh15-PAb4 (left panel probed with primary antibody; right panel probed with primary antibody previously incubated with the peptide antigen; approximate molecular weights indicated for PCDH15-specific signals; asterisks indicate artifact signal). (D, opposite) Light micrographs depicting sections of adult (a and b) and second trimester fetal (c and d) retinas. Sections (a) and (c) were incubated with primary antibody; sections (b) and (d) were incubated with primary antibody pre-absorbed with peptide. Anti-PCDH15 antibody reacts specifically with the inner and outer synaptic layers (ISL and OSL) and nerve fiber layer (NFL) in adult and fetal retinas. Additional reactivity in the region of the outer limiting membrane/photoreceptor cell inner segments (OLM) is observed in adult, but not fetal, retina. Weak binding of the antibody to the retinal pigmented epithelium (PE) is observed in fetal retina. (E, opposite) Light micrographs depicting sections of P8 mouse cochleae (a and b). Section (a) was incubated with primary antibody and section (b) was incubated with primary antibody pre-absorbed with peptide. Thick arrow, anti-Pcdh15 antibody reacts specifically with supporting cells; OSC, outer sulcus cells, SG, spiral ganglion cells; thin arrow, the apical surface of the hair cells.

hypothesize that PCDH15 plays an important role in maintaining normal function of the human inner ear and retina. In the mouse, mutations in *Pcdh15* affect hair cell development in the inner ear. The primary defect appears to be abnormal development of stereocilia, which results in hair cell dysfunction. During later stages, sensory and supporting cell pathology are observed and progress with age to nearly total degeneration of the cochlear neuro-epithelium (7). The role of *PCDH15* in the retina is not clear and to date, no retinal pathology has been

reported in the *Pcdh15* mouse mutant. Studies are underway in our laboratory to determine if *av* mutants show a retinal phenotype consistent with USH1F. Our data also show that *PCDH15* is expressed in brain, kidney, lung and spleen. Since additional abnormalities are not found in persons with USH1F, there may be a level of functional redundancy in some tissues that is provided by other protocadherins.

Analysis of the ORF of *PCDH15* confirms that it is very similar to the ORF deduced from the mouse *Pcdh15* cDNA



sequence. The amino acid sequence of PCDH15 is 94 and 53% identical to the mouse sequence in the extracellular and intracellular domains, respectively. Although the percentage

identity is lower in the intracellular domain, the two proline-rich regions are conserved between species, suggesting that these domains are significant with respect to the function of these proteins.

Protocadherins represent a large family of non-classic cadherins which are structurally and functionally divergent from the classic cadherins. Members of the protocadherin family have been shown to be required for morphogenesis during early development in lower vertebrates (10). In higher vertebrates, based on expression data, protocadherins are thought to be involved in a variety of functions, including neural development, neural circuit formation and formation of the synapse (11).

The function of protocadherins in the mammalian inner ear is not clear, but a survey of the literature and an analysis of the amino acid sequence of PCDH15 lead to an interesting possibility. The process of growth and arrangement of stereocilia on the apical surfaces of hair cells in higher vertebrates is well orchestrated and is a good example of planar polarity. Extensive cytoskeletal re-arrangement takes place during hair cell development.

Stereocilia develop from microvilli on the apical surfaces of hair cells. The microvilli are of uniform size during early embryonic stages; however, as hair cells mature the lateral microvilli grow taller (in a crescent-shaped pattern) while the medial microvilli regress (lateral and medial with respect to the modiolus). This change ultimately leads to the 'V-shaped' bundles that characterize stereocilia, with the tip of the 'V' centered on the kinocilium facing the lateral wall (12).

In *Drosophila*, a characteristic feature of epidermal cells is the projection of bristles that are asymmetrically distributed along the apical surface. Mutations in protocadherin genes, such as *Dachsous* and *Flamingo*, affect this planar polarity (13). Most notably, mutations in *Flamingo* cause randomization of bristle placement, which is broadly reminiscent of the disorganization observed in the placement of stereocilia in mice carrying a mutation in *Pcdh15*. Also, genetic studies in *Drosophila* show that a set of core signaling components (Frizzled receptors and secreted WNT signaling factors) are involved in a signaling pathway that controls planar polarization in a variety of tissues.

The predicted amino acid sequence of PCDH15 contains two well conserved proline-rich regions, which are known to serve as binding sites for profilin or other proteins containing Src homology 3 (SH3) and WW domains (two highly conserved tryptophan residues spaced 20–22 amino acids apart). Profilin regulates polymerization of actin filaments and provides a link between the cytoskeleton and signaling network, while both SH3 and WW domains participate in the assembly of signaling complexes (14). Taken together, we speculate that PCDH15 plays a role in processes that regulate planar polarity in the sensory neuro-epithelium of the inner ear.

A recent report by Raphael *et al.* (15) lends support to our hypothesis. Raphael *et al.* (15) studied the morphology of hair cells from the different alleles of *av* at 15–16 days after birth. They found that in the *Pcdh15<sup>av-2J</sup>* mouse mutant, outer hair cell stereocilia are disorganized, with stereocilia bundles on some of the outer hair cells rotated up to 90° from the normal orientation. Based on this observation, they suggest that the cellular mechanism that regulates orientation of the stereocilia bundle may be affected in the *av* mice.



## MATERIALS AND METHODS

### Family data

Two families segregating for autosomal recessive, profound, congenital deafness and retinitis pigmentosa were ascertained, one in Canada and the second in India. In both families, a genome-wide scan was completed, demonstrating linkage to the USH1F locus. Each participating family member underwent a medical history interview, physical examination including funduscopy and pure tone audiometry. Electroretinography was performed on both affected persons in the Hutterite family. Internal Review Board approval was obtained for this study and informed consent was obtained from all participants.

### Linkage analysis

After isolating DNA from whole blood using a phenol extraction protocol (17), genotyping was completed with 169 STRPs evenly spaced across the human autosomal genome (Screening set 8A, Research Genetics). Both families demonstrated linkage to the USH1F locus on chromosome 10. LOD scores were calculated using either the FASTLINK version of the LINKAGE program package (18,19) or MAPMAKER/HOMOZ (20). The disease allele frequency was set at 0.00075 (21), and the disease was coded as fully penetrant and recessive. An allele frequency of 0.1 for each allele and a 1/1000 phenocopy rate were assumed.

### FISH

FISH was performed using PAC63N4, which contains the human equivalent of the mouse *av* gene. PAC DNA was prepared using the QIAGEN DNA prep kit, following the manufacturer's recommended modification for PACs (Genome Systems). The PAC probe was labeled with biotin 14-dATP by nick translation (BioNick Labeling System 18247-015, Gibco BRL), and the control BAC 70E19 (previously localized to chromosome 10qter) was labeled with digoxigenin. FISH was performed on pro-metaphase chromosomes according to established techniques (22) with minor modifications. Fluorescein-labeled avidin along with biotinylated goat anti-avidin antibody reagents, and rhodamine-labeled anti-digoxigenin along with rabbit anti-sheep and rhodamine-labeled anti-rabbit antibody reagents, were used to detect and amplify probe signals. The slides were counterstained with DAPI. Digital images were collected using a Leitz DMRB microscope controlled by CytoVision ChromoFluor software manufactured and distributed by Applied Imaging Corporation.

### Isolation of *PCDH15* cDNA sequence

We screened a human fetal brain cDNA library (Clontech) with a 4.5 kb mouse *av* cDNA probe using the manufacturer's protocol. Several overlapping cDNA clones were obtained. The cDNA clone with the largest insert (4.3 kb) was sequenced. The remainder of the *PCDH15* cDNA sequence was determined using a combination of different approaches.

We used the mouse *Pcdh15* full-length cDNA sequence to perform BLAST searches against the htgs database to identify BACs containing *PCDH15* genomic sequence. By using the

cDNA sequence, we determined the genomic structure of *PCDH15*. To clone the missing 3' end (~2.5 kb), we completed 3'-RACE and then verified the predicted result by RT-PCR and sequencing.

### RT-PCR analysis

We performed reverse transcription reactions with Superscript reverse transcriptase (Gibco BRL) following the manufacturer's protocol. Total RNA isolated from different human tissues (Clontech) was used, in addition to cochlear RNA isolated from a 19-week-old fetus. In general, PCR conditions were: 94°C for 2 min, followed by 30 cycles of 94°C for 30 s, 55°C for 30 s and 72°C for 1 min. The annealing temperature was adjusted based on the  $T_m$  of the primers. The primers used for RT-PCR were: forward, 5'-GGAGCCCAGAAGTGAAGCAC-3'; and reverse, 5'-TTTTTCTGAAACACTGGGGG-3'.

### RACE

We used the Marathon-Ready cDNA Kit (Clontech) for 5'- and 3'-RACE. RACE template synthesis was carried out using poly(A)<sup>+</sup> RNA from fetal brain, pooled from 10 male/female Caucasians, aged 21–30 weeks, and adult retina, pooled from 76 male/female Caucasians, aged 16–75 years (Clontech) following the manufacturer's protocol. We used the Advantage 2 PCR Kit (Clontech) for both first and second rounds of PCR. The cycling parameters were as follows: 94°C for 30 s, 68°C for 4 min. Products were separated on 1% agarose gels, cloned into the pCR-TOPO vector (Invitrogen) and sequenced. The gene-specific primers used for 5'-RACE were GSP1, 5'-GCGAGTCTTATCTTCATAGTTGAGCCTCTTCCT-3'; and GSP2, 5'-GTGAGCTCATTCCTGTGGCATAGTAGC-3'. Gene-specific primers used for 3'-RACE were GSP3, 5'-AAGG-GACTGAGCGGCAAAGCCGATGTAC-3'; and GSP4, 5'-CT-CCGTGGTCAATCAGCTGGATATGCAAG-3'.

### Mutation detection

*SSCP*. *PCDH15* exons 1–32 were amplified from genomic DNA from family members and a normal-hearing, unrelated control using primers located in the flanking introns (Table 1). PCR products were resolved on polyacrylamide gels.

*Sequencing*. Exons were amplified from genomic DNA from an affected member of each of the two families and a normal-hearing, unrelated control. PCR products were gel-purified and sequenced in both directions using the ABI 373A Dye terminator cycle sequencing system (Perkin Elmer) with the primers used for PCR. Sequences were compared to our cDNA sequence data for *PCDH15*. Exons in which mutations were detected were sequenced in all other persons in both pedigrees.

### Sequence analysis

We used Applied Biosystems DyeDeoxy terminator kit to perform sequencing reactions and the ABI 373 (Perkin Elmer) to resolve the products. The raw sequence data were aligned and compared with *PCDH15* cDNA sequence using the Sequencer program (Gene Codes). The nucleotide sequence data were compared with other sequences in

**Table 1.** *PCDH15* primers

Exon	Exon size (bp)	PCR product size (bp)	cDNA position	Forward primers (5'→3')	Reverse primers (5'→3')
1	355	524	1–355	gtctctgtatgtgctgcca	ttctgtggttcaactgctgc
2	119	242	356–474	aaggcttttctgtgctgga	gctcgcctctaaaggtcaagcta
3	66	174	475–540	gtgccctgcagcaattat	gaattaaactgaagaaaaccctc
4	161	429	541–701	aaactgattgagccagcc	tgtccctctcttctcattc
5	156	267	702–857	cgagtccttgacagtatga	tcaacagaagacagagagaga
6	120	283	858–977	catttctggtgagcagttga	tctggtctggaagtactgaata
7	111	198	978–1088	cattcaataatctgaagtctgtatc	tactcataaattcacagaagaaat
8	171	383	1089–1259	atgtttccaggctggtatc	acatgatcccattgggtttt
9	109	223	1260–1368	aatcgcgctgaatgaaactc	ttccttggaaltgagagaatttg
10	113	277	1369–1481	cctcagctgatgaaggaaa	tgccacagtagcgtctacagatt
11	207	491	1482–1688	tgcataaaaagtgaactcca	atctgcaagctgaaaaggaa
12	135	358	1689–1823	ctttcacgtggattttgct	tttcccccaagtcattgat
13	150	247	1824–1973	atttcagaacatctactaagtgtga	tgacatgtaataacagctttg
14	194	334	1974–2167	aagggaagtctcaccacaca	aatactgccgcgctcttta
15	133	125	2168–2300	ccatctgcaactgtatattgaa	tagatlaataaaacagcaccacacc
16	80	185	2301–2380	gtggcgccatcaattac	ctaacagtactgtgtgaca
17	94	181	2381–2474	aagaagactctcttctgaca	ccttcacagggagcactactc
18	129	292	2475–2603	gctcctctcatttaagtcttg	ttgaagaataccagcagctca
19	306	508	2604–2909	atttctcttagaggcca	aatlttgccacaaaaccct
20	225	363	2910–3134	gctgtcctagcactaacgc	tacagagagcaaaagcaggca
21	117	366	3135–3251	ttcctctgaggtgccagtct	tttctgtctgtgattcgg
22	141	327	3252–3392	cgattttcactctaaaagacca	tgctgtactctgtaagccaa
23	113	220	3393–3505	ttgtctgttactactgttcttac	atgccctaacaattctgtctttt
24	110	237	3506–3617	tttctcaattttctgtgaacg	tggttgatggtgagaacacaa
25	141	346	3618–3756	tgtcaattcatgcatcactct	tgatcttctatgtgtccactga
26	128	209	3757–3884	gcatcgtttctgtcctcca	gcttatctgcaaaacctgagc
27	216	384	3885–4100	catttagagggctttattgtg	tcgtgactactcccttctctg
28	89	351	4101–4189	tcagaaaccactgtgtctatgc	gcacactcgaagcctaaacc
29	177	282	4190–4366	ttttactcccagaagccca	gttgctattgtaaccaagagc
30	228	319	4367–4594	accttaagcccataatgagc	cagctgtgtttcaattagagaa
31	156	309	4595–4750	ccctgataactggaccccat	ccacacagaattcagtaaaacc
32	2069	2444	4751–6819	gctgtgtcacaactgtttctct	aagggaagggaagcacaat

GenBank using BLAST (23). The PSORT II program (<http://psort.nibb.ac.jp:8800>) predicted the cytoplasmic, transmembrane and extracellular domains, and the ProfileScan program ([http://www-isrec.isb-sib.ch/software/PRScan\\_form.html](http://www-isrec.isb-sib.ch/software/PRScan_form.html)) identified the cadherin repeats. GenBank was the source of sequences of other mouse cadherin protein sequences. We used CLUSTAL W (<http://www.ebi.ac.uk/clustalw>) to generate the phylogenetic tree using the program's default settings and viewed using Njplot (24). The analysis was restricted to the cytoplasmic domain to avoid the confounding effect caused by variation in the number of cadherin repeats. Mouse and human cadherin sequences from GenBank were analyzed with PSORT II to predict the cytoplasmic domain.

### Northern blot analysis

We obtained human Poly(A)<sup>+</sup> RNA from Clontech and performed northern blot analysis using a 4 kb fragment of *PCDH15* cDNA as a probe, as described previously (25). We washed the membranes with a final stringency of 0.2× SSC/0.1% SDS/50°C for 1 h. For control probe β-actin, we raised the wash temperature to 65°C. Filters were exposed to Kodak MS film from several hours to several days.

### Western blot analysis

We used western blots containing proteins from adult human brain, lung and kidney (Research Genetics), and probed them with affinity-purified antibodies (Pcdh15-PAb4) raised against the



mouse Pcdh15 peptide sequence (TEDAHESEKEGGH-RDTLIV). The antibodies were raised in rabbits. Western blot analysis was performed following standard protocols (26).

### Immunohistochemistry

Tissues from human adult and fetal retina were fixed in 4% paraformaldehyde in 100 mM sodium cacodylate pH 7.4. After 2–4 h of fixation, eyes were transferred to 100 mM sodium cacodylate, infiltrated and embedded in acrylamide, as described previously (27). Tissues were subsequently embedded in OCT and sectioned to a thickness of 6–8  $\mu\text{m}$ . We used as a primary antibody the same antibody that was used in the western blot. The secondary antibody was goat anti-rabbit IgG conjugated to biotin (Vector Laboratories), followed by avidin biotin complex labeled with horseradish peroxidase (HRP) (ABC Elite kit, Vector Laboratories). HRP was visualized using the Vector VIP substrate kit (Vector Laboratories) with incubation for 2–5 min at room temperature (RT). Adjacent sections were incubated with pre-absorbed primary antibody alone to serve as negative controls.

The cochleae used in this study were obtained from mice 8 days after birth (P8). We chose this time point because the organ of Corti is well developed and *Pcdh15* is known to be expressed. To obtain the cochleae, the mice were sacrificed and the inner ears were dissected. Each cochlear capsule was partly opened and immersed in 4% paraformaldehyde in PBS for 1 h at RT. After rinsing three times with PBS at RT, each cochlea was decalcified with 0.35 M EDTA in 0.01 M sodium phosphate buffer (pH 7.2) overnight at 4°C. Tissues were rinsed in PBS, dehydrated through a graded series of alcohols, cleared in histoclear, and embedded in paraffin using standard procedure.

Sections were cut at 4  $\mu\text{m}$  in the modiolar plane, and two to four sections were mounted on each slide. Sections were deparaffinized, rehydrated and treated with 0.3% hydrogen peroxide to quench endogenous peroxidase activity. Sections were blocked with 1% normal goat serum for 30 min, then incubated overnight in primary antisera at 4°C at the optimal dilution as determined by titration studies. Forty sections (10 separate microscope slides, each with four sections on it) were incubated with the primary antisera simultaneously. Controls consisted of incubating sections in normal serum lacking the primary antisera or pre-absorbing with 10-fold excess peptide antigen TEDAHESEKEGGH-RDTLIV.

After 24 h, sections were rinsed in PBS, incubated in biotinylated goat anti-rabbit IgG for 20 min at RT, rinsed in PBS, and incubated for 30 min with avidin–biotin HRP complex (ABC, Vector labs). To visualize the binding sites of the primary antibody, sections were incubated in a couplin jar containing 3,3'-diaminobenzidine-HCl (DAB)-H<sub>2</sub>O<sub>2</sub>.

### GenBank accession nos

*PCDH15* cDNA, accession no. AY029205; mouse *Pcdh15*, AF281899; *PCDH15* exons 1–32, AL356114, AL353784, AL360214, AC013737, AC024073, AC027671, AC021350, AC016817, AL365496.

### ACKNOWLEDGEMENTS

We would like to thank H. Dakappagari for technical assistance. This research was supported by grants EY11515 to G.S.H., RO1-DC03420 to R.P.W. and RO1-DC02842 to R.J.H.S.. C.L.M. was supported by NIH training grant HD07104.

### REFERENCES

- Smith, R.J.H., Berlin, C., Hejtmanek, J.F., Keats, B., Kimberling, W.J., Lewis, R.A., Möller, C.G., Pelias, M.Z. and Tranebjærg, L. (1994) Clinical diagnosis of the Usher syndromes. *Am. J. Med. Genet.*, **50**, 32–38.
- Astuto, L.M., Weston, M.D., Carney, C.A., Hoover, D.M., Cremers, C.W.R.J., Wagenaar, M., Moller, C., Smith, R.J.H., Piek-Dahl, S., Greenberg, J. *et al.* (2000) Genetic heterogeneity of Usher syndrome: analysis of 151 Usher I families. *Am. J. Hum. Genet.*, **67**, 1569–1574.
- Wayne, S., Der Kaloustian, V.M., Schloss, M., Polomeno, R., Scott, D.A., Sheffield, V.C. and Smith, R.J.H. (1997) Localization of Usher syndrome type 1F to chromosome 10. *Am. J. Hum. Genet.*, **61**, A300.
- Hostetler, J.A. (1985) History and relevance of the Hutterite population for genetic studies. *Am. J. Med. Genet.*, **22**, 453–462.
- Lowry, R.B., Morgan, K., Holmes, T.M. and Gilroy, S.W. (1985) Congenital anomalies in the Hutterite population: a preliminary survey and hypothesis. *Am. J. Med. Genet.*, **22**, 545–552.
- Alagramam, K.N., Zahorsky-Reeves, J., Wright, C.G., Pawlowski, K.S., Erway, L.C., Stubbs, L. and Woychik, R.P. (2000) Neuroepithelial defects of the inner ear in a new allele of the mouse mutation Ames waltzer. *Hear. Res.*, **148**, 181–190.
- Alagramam, K.N., Murcia, C.L., Kwon, H.Y., Pawlowski, K.S., Wright, C.G. and Woychik, R.P. (2001) The mouse Ames waltzer hearing-loss mutant is caused by mutation of *Pcdh15*, a novel protocadherin gene. *Nat. Genet.*, **27**, 99–102.
- Bolz, H., von Brederlow, B., Rez, A., Bryda, E.C., Kutsche, K., Nothwang, H.G., Seeliger, M., Cabrera, M., Vila, M.C., Molina, O.P. *et al.* (2001) Mutation of CDH23, encoding a new member of the cadherin gene family, causes Usher syndrome type 1. *Nat. Genet.*, **27**, 108–112.
- Wu, Q. and Maniatis, T. (2001) Comparative DNA sequence analysis of the mouse and human protocadherin gene clusters. *Genome Res.*, **11**, 389–404.
- Kim, S.H., Yamamoto, A., Bouwmeester, T., Agius, E. and Robertis, E.M. (1998) The role of paraxial protocadherin in selective adhesion and cell movements of the mesoderm during *Xenopus* gastrulation. *Development*, **125**, 4681–4690.
- Suzuki, S.T. (2000) Recent progress in protocadherin research. *Exp. Cell Res.*, **261**, 13–18.
- Pujol, R., Lavingne-Rebillard, M. and Lenoir, M. (1998) Development of sensory and neural structures in mammalian cochlea. In Rubel, E.W., Popper, A.N. and Fay, R.R. (eds), *Development of the Auditory System*. Springer, NY, pp. 146–192.
- Eaton, S. (1997) Planar polarization of *Drosophila* and vertebrate epithelia. *Curr. Opin. Cell Biol.*, **9**, 860–866.
- Sudol, M. (1998) From Src homology domains to other signaling modules: proposal of 'protein recognition code'. *Oncogene*, **17**, 1469–1474.
- Raphael, Y., Kobayashi, K.N., Dootz, G.A., Beyer, L.A., Dolan, D.F. and Burmeister, A. (2001) Severe vestibular and auditory impairment in three alleles of Ames waltzer (*av*) mice. *Hear. Res.*, **151**, 237–249.
- Bork, J.M., Peters, L.M., Riazuddin, S., Bernstein, S.L., Ahmed, Z.M., Ness, S.L., Polomeno, R., Ramesh, A., Schloss, M., Srisailapathy, C.R.S. *et al.* (2001) Usher syndrome 1D and nonsyndromic autosomal recessive deafness DFNB12 are caused by allelic mutations of the novel cadherin-like gene CDH23. *Am. J. Hum. Genet.*, **68**, 26–37.
- Grimberg, J., Nawoschik, S., Belluscio, L., McKee, R., Turck, A. and Eisenberg, A. (1989) A simple and efficient non-organic procedure for the isolation of genomic DNA from blood. *Nucleic Acids Res.*, **17**, 8390.
- Lathrop, G.M. and Lalouel, J.M. (1984) Easy calculations of LOD scores and genetic risks on small computers. *Am. J. Hum. Genet.*, **36**, 460–465.
- Schaffer, A.A. (1996) Faster linkage analysis computations for pedigrees with loops or unused alleles. *Hum. Hered.*, **46**, 226–235.
- Kruglyak, L., Daly, M.J. and Lander, E.S. (1995) Rapid multipoint linkage analysis of recessive traits in nuclear families, including homozygosity mapping. *Am. J. Hum. Genet.*, **56**, 519–527.
- Zbar, R.I., Ramesh, A., Srisailapathy, C.R.S., Fukushima, K., Wayne, S. and Smith, R.J.H. (1998) Passage to India: the search for genes causing

- autosomal recessive nonsyndromic hearing loss. *Otolaryngol. Head Neck Surg.*, **118**, 333–337.
22. Pinkel, D., Straume, T. and Gray, J.W. (1986) Cytogenetic analysis using quantitative, high-sensitivity, fluorescence hybridization. *Proc. Natl Acad. Sci. USA*, **83**, 2934–2938.
23. Altschul, S.F., Madden, T.L., Schaffer, A.A., Zhang, J., Zhang, Z., Miller, W. and Lipman, D.J. (1997) Gapped BLAST and PSI-BLAST: a new generation of protein database search programs. *Nucleic Acids Res.*, **25**, 3389–3402.
24. Perriere, G. and Gouy, M. (1996) WWW-query: An on-line retrieval system for biological sequence banks. *Biochimie*, **78**, 364–369.
25. Bultman, S.J., Michaud, E.J. and Woychik, R.P. (1992) Molecular characterization of the mouse agouti locus. *Cell*, **71**, 1195–1204.
26. Sasse, J. and Gallagher, S.R. (1991) Detection of proteins. In Ausubel, F.M., Brent, R., Kingston, R.E., Moore, D.D., Seidman, J.G., Smith, J.A. and Struhl, K. (eds), *Current Protocols*, John Wiley & Sons, Vol. 2, pp. 10.7.1–10.8.16.
27. Mullins, R., Johnson, L., Anderson, D. and Hageman, G. (1997) Characterization of drusen-associated glycoconjugates. *Ophthalmology*, **104**, 288–294.